# Magnetic resonance imaging of the jugular foramen.

D L Daniels, J F Schenck, T Foster, H Hart, Jr, S J Millen, G A Meyer, P Pech and V M Haughton

*AJNR Am J Neuroradiol* 1985, 6 (5) 699-703
http://www.ajnr.org/content/6/5/699

# Magnetic Resonance Imaging of the Jugular Foramen

David L. Daniels[1]
John F. Schenck[2]
Thomas Foster[2]
Howard Hart, Jr.[2]
Steven J. Millen[3]
Glenn A. Meyer[4]
Peter Pech[1]
Victor M. Haughton[1]

**The jugular foramen in normal volunteers was studied with 1.5 T magnetic resonance (MR) systems in 3-mm-thick head- and surface-coil images. Anatomic sections through cadaver heads were correlated with the MR images to identify the jugular bulb and the course of cranial nerves IX–XI. Sagittal images were more useful than coronal or axial to show the course of these nerves through the skull base. MR demonstrates the anatomic relations of the jugular foramen (except its osseous margins) such that its primary use in evaluating this region can be anticipated.**

Although computed tomography (CT) is useful for demonstrating the jugular foramen, it fails to demonstrate cranial nerves IX–XI consistently. Since effective magnetic resonance (MR) demonstration of cranial nerves in the internal auditory canals and cavernous sinuses has been reported [1, 2], its demonstration of cranial nerves IX–XI can be predicted. MR imaging in the jugular foramen is facilitated by the lack of signal from flowing blood and bone. The purpose of our article is to describe the MR appearance of the normal contents of the jugular foramen.

## Materials and Methods

Four fresh, frozen cadaver heads were embedded with carboxymethyl cellulose gel in styrofoam boxes. The jugular foramina were sectioned using a heavy-duty sledge cryomicrotome (LKB 2250, Gaithersburg, MD) either parallel to the sagittal plane or to planes forming an angle of 0° or +30° to the canthomeatal line (CML) [3]. Anatomic images were obtained by photographing the surfaces of the specimens as they were sectioned.

Five normal volunteers were studied in research General Electric MR scanners with superconducting 1.5 T magnets [4] and head or surface coils. All images were obtained with a spin-warp spin-echo technique [5]. Head-coil imaging included an initial sagittal image for localizing and thin axial (parallel to the CML) and parasagittal sections. A flexible-surface receiver coil 13.5 cm in diameter and tuned to 63.9 MHz was placed over the jugular foramina of the normal volunteers for surface-coil imaging. A 54-cm-diam cylindrical coil, used for body imaging, was used for the radiofrequency transmitter. Surface-coil images were obtained using planes parallel or +30° to the CML and using parasagittal planes. Technical factors for head-coil images included 300–400 msec TR; 14 msec TE; 128 × 256 or 256 × 256 matrices; 1.9 × 1.0 mm and 1.0 × 1.0 mm, respectively, pixel sizes; 25 cm field of view; and 3 and 5 mm slices. Technical factors for surface-coil images included 200–400 msec TR; 19 msec TE; 128 × 256 or 256 × 256 matrices; 1.0 × 0.5 mm and 0.5 × 0.5 mm, respectively, pixel sizes; 12.8 cm field of view; and 3-mm-thick slices.

The MR images of the volunteers and photographs of the anatomic sections (figs. 1–5) were correlated with published anatomic and CT literature [6–12] to identify cranial nerves IX–XI, the jugular vein, and the internal carotid artery.

Received November 28, 1984; accepted after revision February 28, 1985.

Presented at the annual meeting of the American Society of Neuroradiology, New Orleans, February 1985.

This work was supported by a grant from General Electric Medical Systems.

[1] Department of Radiology, Medical College of Wisconsin, Froedtert Memorial Lutheran Hospital, 9200 W. Wisconsin Ave., Milwaukee, WI 53226. Address reprint requests to D. L. Daniels.

[2] General Electric Research and Development Center, Schenectady, NY 12301.

[3] Department of Otolaryngology, Medical College of Wisconsin, Milwaukee, WI 53226.

[4] Department of Neurosurgery, Medical College of Wisconsin, Milwaukee, WI 53226.

*AJNR* 6:699–703, September/October 1985
0195–6108/85/0605–0699

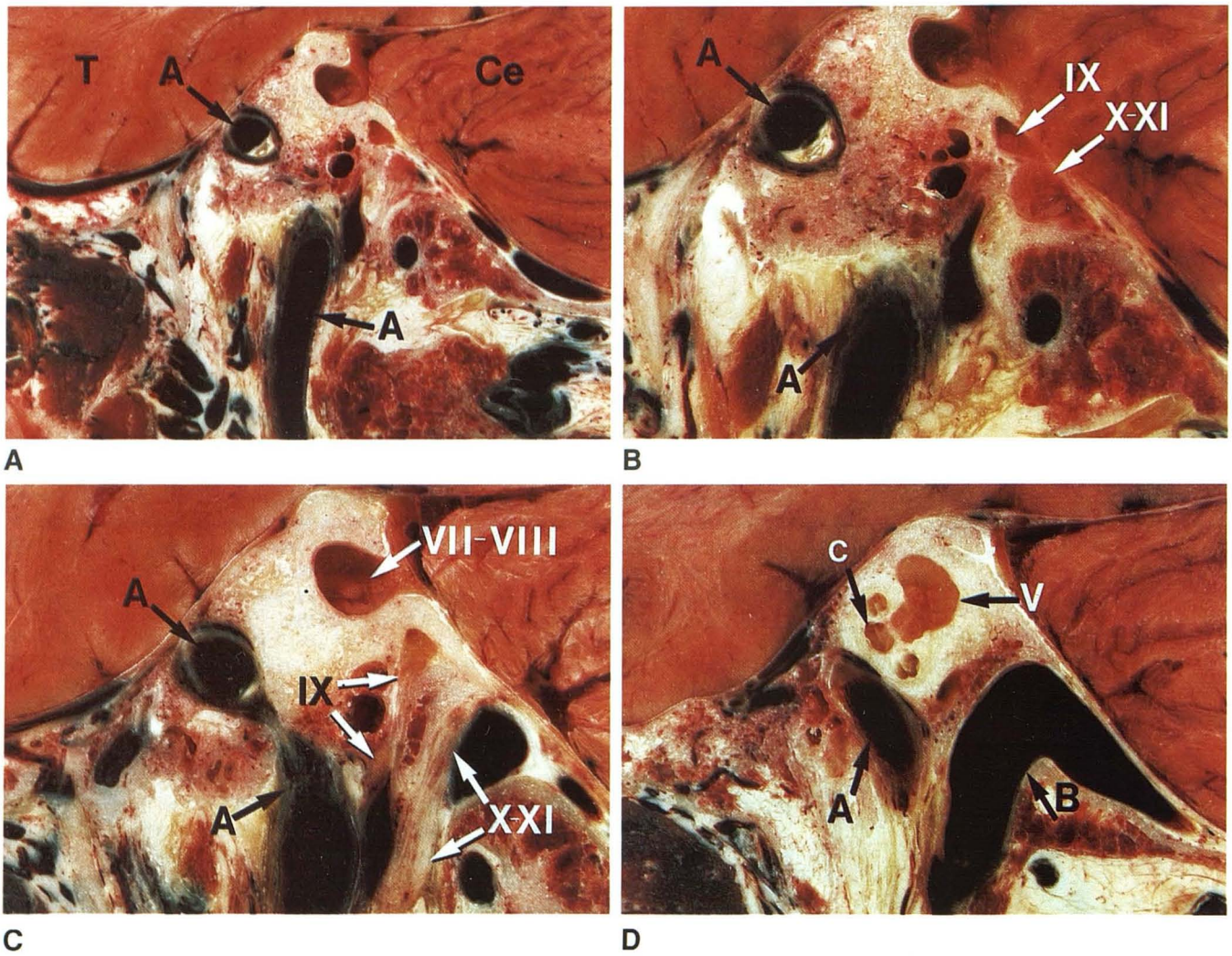


Fig. 1.—Parasagittal cryomicrotomic sections of jugular foramen from medial to lateral. **A**, Cranial nerve IX is in pars nervosa, and cranial nerves X and XI together, in pars vascularis. Segments of internal carotid artery (A) are below and within carotid canal. **B**, Magnification of **A. C**, Cranial nerves IX and X–XI, separated by thin spicule of bone, have oblique and nearly parallel course through skull base. **D**, Jugular bulb (B) and internal carotid artery. T = temporal lobe; Ce = cerebellum; VII–VIII = cranial nerves in the internal auditory canal; V = vestibule; C = cochlea.

## Results and Discussion

The jugular foramen consists of the pars nervosa (glossopharyngeal [IX] nerve and inferior petrosal sinus) and, posterior to it, the pars vascularis (vagus [X] and spinal accessory [XI] nerves and jugular bulb). A plane of section of +30° to the CML and dynamic scanning techniques are used with CT to identify cranial nerves in the jugular foramen [6].

In cryomicrotomic sections, cranial nerves IX–XI have a constant position in the jugular foramen (figs. 1 and 4). In a plane of +30° to the CML (nearly parallel to the clivus), these nerves have an almost straight lateral course from the medulla to the endocranial opening of the jugular foramen (fig. 4). In the foramen, IX is anterior and X and XI posterior. Sagittal sections show cranial nerve IX in a dural sheath in the jugular foramen and then from the skull base anteroinferiorly to the tongue and pharynx (fig. 1). Cranial nerves X and XI, in a common dural sheath behind IX, lie anteromedial to the jugular bulb and then course anteroinferiorly below the skull base. They may appear slightly wider at the endocranial opening of the foramen. Through the skull base they have a slightly oblique course nearly parallel to cranial nerve IX. Cranial nerve X and one branch of XI terminate in the carotid sheath; one branch of XI terminates in the neck muscles.

On MR images structures that have a signal intensity intermediate between fat and cerebrospinal fluid (figs. 2, 3, and 5) have been identified that correspond to cranial nerves IX–XI in the cryomicrotomic sections. The jugular bulb can be demonstrated on parasagittal images.

Surface-coil images demonstrate the cranial nerve anatomy better than do head-coil images. The higher signal-to-noise ratio offered by surface coils permits smaller pixel sizes. The cisternal segments of cranial nerves IX–XI are effectively

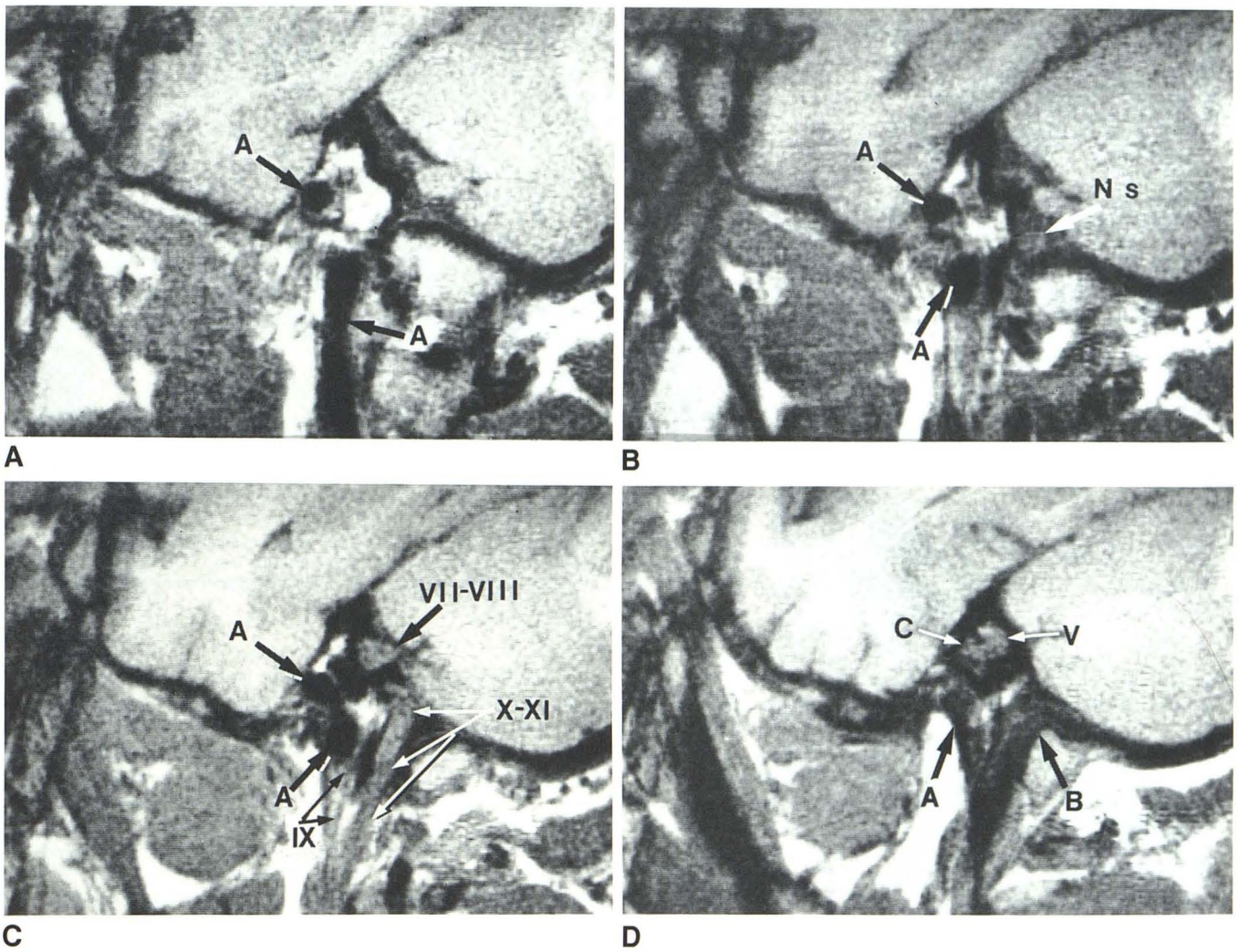


Fig. 2.—Parasagittal surface-coil MR scans, 400 msec TR, 19 msec TE, 256 × 256 matrix, 205 sec scan time, 3 mm thick, from medial to lateral corresponding to anatomic sections in fig. 1. **A** and **B**, Segments of internal carotid artery (A) have negligible signal. Ns = cranial nerves. **C**, Cranial nerves IX and X–XI, osseous foramen (negligible signal), and fat (high-intensity signal). Cranial nerves VII and VIII are identified in internal auditory canal. **D**, Internal carotid artery and jugular bulb (B) and vein have negligible signal. C = cochlea; V = vestibule.

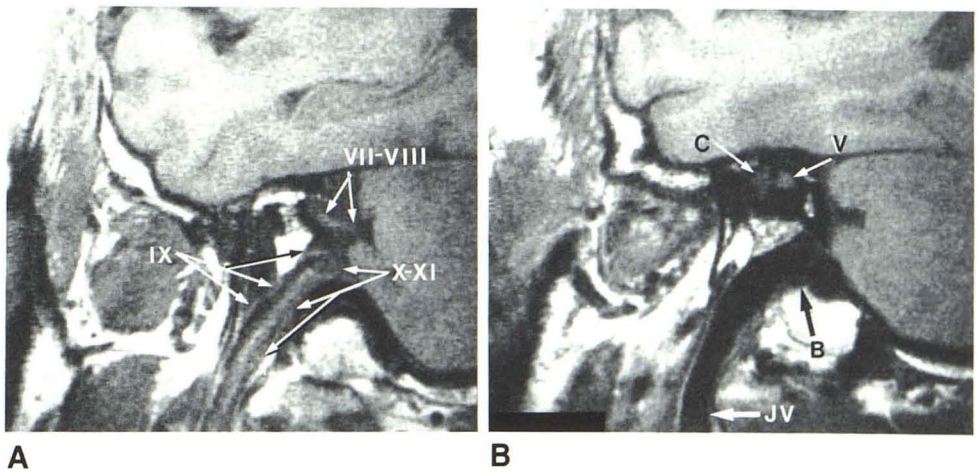


Fig. 3.—Parasagittal surface-coil MR images, 400 msec TR, 19 msec TE, 256 × 256 matrix, 205 sec scan time, 3 mm thick. Cranial nerves IX and X–XI in skull base (**A**) and jugular bulb (B) just lateral to cranial nerves IX–XI (**B**). C = cochlea; V = vestibule; JV = jugular vein.

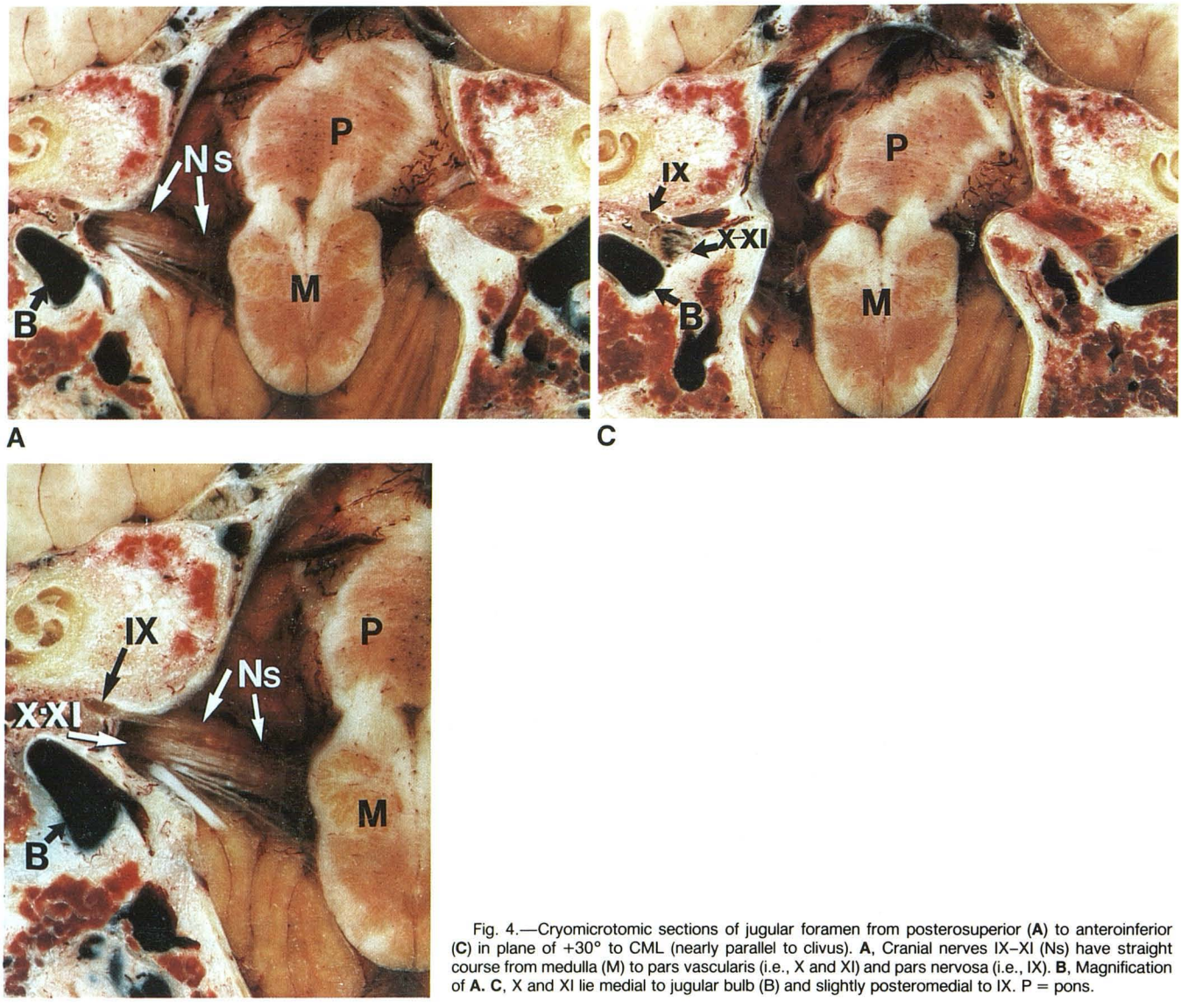


Fig. 4.—Cryomicrotomic sections of jugular foramen from posterosuperior (**A**) to anteroinferior (**C**) in plane of +30° to CML (nearly parallel to clivus). **A**, Cranial nerves IX–XI (Ns) have straight course from medulla (M) to pars vascularis (i.e., X and XI) and pars nervosa (i.e., IX). **B**, Magnification of **A. C**, X and XI lie medial to jugular bulb (B) and slightly posteromedial to IX. P = pons.

shown in the axial plane, the endocranial segments of the nerves in a plane of +30° to the CML. Parasagittal surface-coil images consistently show the intraforaminal and extracranial course of these nerves (figs. 2 and 3).

High-resolution surface-coil MR images provide consistently better demonstration of cranial nerves IX–XI in the jugular foramen and in extracranial tissues without a contrast agent than do CT images [6]. Because it demonstrates the individual nerves, MR should effectively exclude tumor in the jugular foramen when IX, X, or XI nerve signs are present. CT reliably demonstrates intraforaminal tumors only when the osseous margins are eroded. A series of foraminal tumors should be studied with MR to determine if T1 and T2 measurements or different pulse sequences will increase the specificity of neuroradiologic diagnosis in jugular foramen lesions.

ACKNOWLEDGMENTS

We thank Cecil Hayes, William A. Edelstein, Ann Shimakawa, and Laurie Dunk for help in this study.

REFERENCES

1. Daniels DL, Herfkins R, Koehler PR, et al. Magnetic resonance imaging of the internal auditory canal. *Radiology* **1984**;151:105–108
2. Daniels DL, Pech P, Mark L, Pojunas K, Williams AL, Haughton VM. Magnetic resonance imaging of the cavernous sinus. *AJNR* **1985**;6:187–192, *AJR* **1985**;144:1009–1014
3. Rauschning W, Bergstrom K, Pech P. Correlative craniospinal anatomy studies by computed tomography and cyromicrotomy. *J Comput Assist Tomogr* **1983**;7:9–13

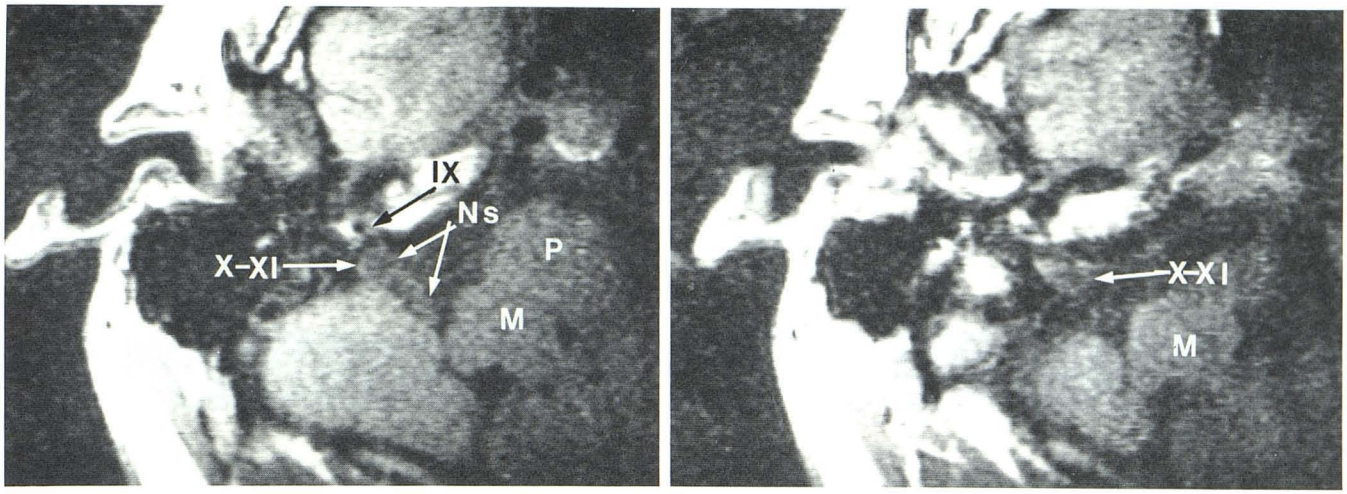


A B

Fig. 5.—Surface-coil MR images, 200 msec TR, 19 msec TE, 128 × 128 matrix, 52 sec scan time, 3 mm thick, of jugular foramen in plane of +30° to CML corresponding to anatomic sections in fig. 4. **A**, Endocranial course of cranial nerves IX–XI (Ns). IX lies in pars nervosa and X–XI in pars vascularis. Jugular bulb is not seen well. **B**, Slightly anteroinferior to **A.** Again, X–XI can be seen. P = pons; M = medulla.

4. Bottomley PA, Hart HR, Edelstein WA, et al. Anatomy and metabolism of the normal human brain studied by magnetic resonance at 1.5 Tesla. *Radiology* **1984**;150:441–446
5. Edelstein WA, Bottomley PA, Hart HR, Smith LS. Signal, noise and contrast in nuclear magnetic resonance (NMR) imaging. *J Comput Assist Tomogr* **1983**;7:391–401
6. Daniels DL, Williams AL, Haughton VM. Jugular foramen: anatomic and computed tomographic study. *AJNR* **1983**;4:1227–1232, *AJR* **1984**;142:153–158
7. Lo WWM, Solti-Bohman LG, Lambert PR. High-resolution CT in the evaluation of glomus tumors of the temporal bone. *Radiology* **1984**;150:737–742
8. Lo WWM, Solti-Bohman LG. High-resolution CT of the jugular foramen: anatomy and vascular variants and anomalies. *Radiology* **1984**;150:743–747
9. Strickler JM. New and simple techniques for demonstration of the jugular foramen. *AJR* **1966**;97:601–606
10. Gray H. *Anatomy of the human body*. Philadelphia: Lea & Febiger, **1966**
11. Rhoton AL, Buza RC. Microsurgical anatomy of the jugular foramen. In: Rand RW, ed. *Microneurosurgery*, 2d ed. St. Louis: Mosby, **1978**:252–264
12. Di Chiro G, Fisher RL, Nelson KB. The jugular foramen. *J Neurosurg* **1964**;21:447–460